Simultaneous BTD (WV6.2-IR10.8) Anomaly and Above-anvil Ice Plume Observed above the Storm of 06 July 2010, North Italy

Mária Putsay[1], Martin Setvák[2], André Simon[1], Jochen Kerkmann[3]

[1]Hungarian Meteorological Service, [2]Czech Hydrometeorological Institute, [3]EUMETSAT

putsay.m@met.hu

INTRODUCTION

The brightness temperature difference (BTD) of the MSG bands WV6.3 and IR10.8 is typically positive above cold storm anvils (e.g. Fritz and László, 1993; Ackerman 1996; Schmetz et al., 1997; Setvák et al., 2007 and 2008).

This effect can be attributed either to a warm water vapor (lower-stratospheric moisture, LSM) above the tops of convective storms, or to scattering effects atop storm anvils. The first effect (LSM) seems to play a more significant role (Setvák et al., 2008), most of the positive BTD observations can be attributed to the warmer LSM.

The positive BTD can be either closely correlated to the IR brightness temperature, or exhibit various local 'BTD anomalies'. The first case relates to a semi-homogenous LSM layer being advected from elsewhere, while the second case represents a manifestation of possible local source of LSM – the storm itself (Setvák, 2010 – Part 2).

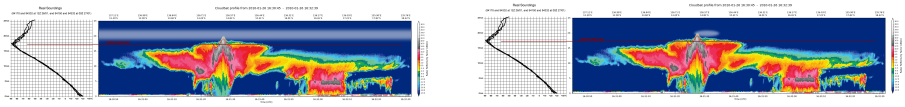

Cross sections of a mature thunderstorm penetrated into the lower stratosphere with a) homogeneus lower-stratospheric moisture above it, b) moisture injected by the storm above the anvil (illustration from Setvak (2010 – Part 2).

The development of such above-anvil moisture plumes was successfully simulated by Wang (2007). Rise and decay of intense overshooting tops trigger gravity waves and in some conditions plumes may form due to the gravity wave breaking mechanism.

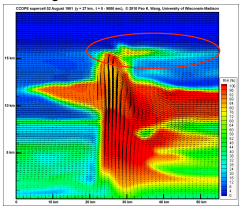

Example of numerical simulation of plume generating thunderstorm (Wang, 2007)

OBSERVED CLOUD TOP FEATURES

The 06 July 2010 case is unique by a simultaneous occurrence of the BTD anomaly and a nearby ice plume.

The BTD(WV6.2-IR10.8) anomaly formed in close vicinity of the above-anvil ice plume, with some delay after the ice plume formation. At certain phase of the evolution, the BTD anomaly (BTD > 2 K) resembles a plume-like feature, but for most of the time it has an irregular, rather oval shape.

At the earlier stages of the storm evolution, the BTD field more or less indicates the pre-existing moist layer above the storm, manifested by close correlation of the BTD and BT10.8 fields (Fig. 1).

BTD anomaly appears about 45 minute later then the longer-lived ice plume started to evolve. The first significant BTD anomaly occurs on the northern flank of the storm, north of the ice plume (Fig. 2).

The BTD anomaly for a short period of time (~ 20-30 minutes) resembles a distinct plume-like feature, oriented similarly as the ice plume (see Fig. 3). The north outline of the ice plume defines the south outline of the BTD anomaly.

From 17:25 UTC on, the area of high BTD values (BTD anomaly) begins to lose its plume-like shape, and transforms back into an irregular, more or less oval region north of the plume. The north outline of the ice plume does not define the south outline of the BTD anomaly anymore. At 17:40 UTC (Fig. 4) the shape, extent and position of the BTD anomaly have nothing common with the ice plume.

In late stages, for example at 18:20 UTC (Fig. 5) the high BTD values (indicated by yellow circle) are above the older dissipating cell only, where we are looking at "bare" (not covered by an ice plume) cloud top. The young cell at the south-west (indicated by red circle) exhibits only very low BTD values. In similar cases the overshooting top detection based on 'BTD method' (Bedka, 2011) would fail for the active parts of the storm (the BTD algorithm expects higher positive BTD values).

METEOSAT-8 HRV/IR10.8 blended images	*METEOSAT-8 BTD(WV6.2-IR10.8) images*
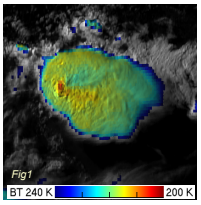 *Fig1* BT 240 K … 200 K	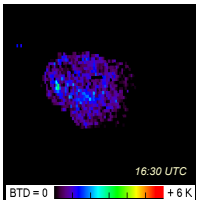 *16:30 UTC* BTD = 0 … + 6 K
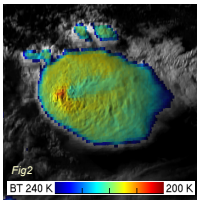 *Fig2* BT 240 K … 200 K	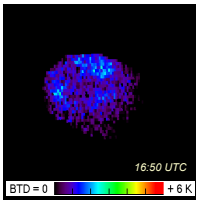 *16:50 UTC* BTD = 0 … + 6 K
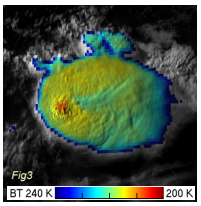 *Fig3* BT 240 K … 200 K	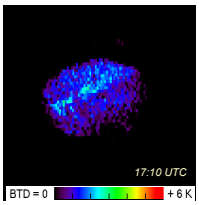 *17:10 UTC* BTD = 0 … + 6 K
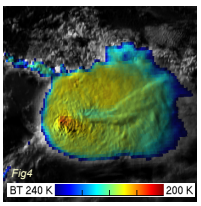 *Fig4* BT 240 K … 200 K	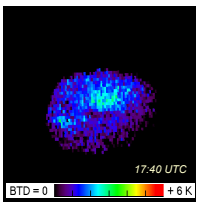 *17:40 UTC* BTD = 0 … + 6 K
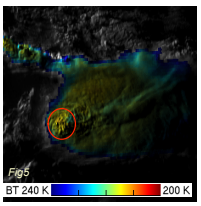 *Fig5* BT 240 K … 200 K	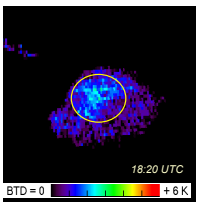 *18:20 UTC* BTD = 0 … + 6 K

DISCUSSION

The main question is whether the BTD anomaly was caused by an above-anvil water vapor plume originating from the storm, or by scattering effects atop the storm anvil, related to storm-top microphysics.

We cannot exclude the storm-top microphysics being responsible for the BTD anomaly, however we failed finding any traces of the BTD anomaly being reflected in the anvil top morphology or microphysics as determined from the 3.9 micron band. Neither the brightness temperate differences of other IR channel pairs (e.g. the IR9.7-IR13.4, or IR13.4-IR10.8) showed any trace of the BTD (WV6.2-IR10.8) anomaly structure. This makes the water vapor mechanism being more likely responsible as the explanation for this feature.

The BTD plume was oriented similarly as the ice plume, supporting the theory that both might have the same origin in the gravity wave breaking mechanism. However, the shape of the BTD anomaly was mostly irregular, showing the plume-like shape only for a short period of time.

If the BTD plume was indeed a WV plume injected by the storm, then the distinction between these two plumes (water vapor and ice plume) might be either in their altitude (and thus surrounding temperature, with the ice plume being formed in the cooler environment), or in the saturation of the plume area (the more humid air forming an ice plume), or in the specifics of the mechanism forming these two plumes (Wang, 2007).

Further studies are needed to better understand the nature and mechanisms forming the BTD anomalies as this case. Anyhow, this is the first case when a significant plume-like BTD anomaly was observed in such proximity to the above-anvil ice plume. Also, as the BTD (WV6.2-IR10.8) (or similar for other satellites) are being used frequently in various nowcasting algorithms, proper understanding of its nature is essential for refining or improving these techniques and satellite-derived products.

REFERENCES

Ackerman S.A., 1996: Global satellite observations of negative brightness temperature differences between 11 and 6.7 micron. *J. Atmos. Sci.*, 53 2803-2812.

Bedka K., 2011: Overshooting cloud top detections using MSG SEVIRI Infrared brightness temperatures and their relationship to severe weather over Europe. *Atmos. Res.* 99 175-189.

Fritz S., László I.. 1993: Detection of water vapor in the stratosphere over very high clouds in the tropics. *J. Geophys. Res.* 98 22959- 22967.

Schmetz J., Tjemkes S.A., Gube M., van de Berg L., 1997: Monitoring deep convection and convective overshooting with METEOSAT. *Adv. Space Res.* 19 433-441.

Setvák M., Rabin R.M., Doswell C.A., Levizzani V., 2003: Satellite observations of convective storm tops in the 1.6, 3.7 and 3.9 μm spectral bands. *Atmos. Res.* 67–68, 607–627.

Setvák M., Rabin R.M., Wang P.K., 2007: Contribution of the MODIS instrument to observations of deep convective storms and stratospheric moisture detection in GOES and MSG imagery. *Atmos. Res.*, 83 505-518.

Setvák M. Lindsey D.T. Rabin R.M., Wang P.K. Demeterova A., 2008: Indication of water vapor transport into the lower stratosphere above midlatitude convective storms: Meteosat Second Generation satellite observations and radiative transfer model simulations. *Atmos. Res*, 89 170-180.

Setvák, M., Ronge, L., Kaňák, J. 2009: Sandwich product – blending the HRV and IR10.8 BT imagery. In the Convection Working Group, Documentation, http://www.convection-wg.org/sandwich.php.

Setvák, 2010: Satellite observations of storm tops, Part 1 and Part 2. In the EUMETSAT Data and Products, Online Training Library, http://www.eumetsat.int/.

Wang P.K., 2007: The thermodynamic structure atop a penetrating convective thunderstorm. *Atmos. Res.*, 83 254-262.